

AD-A095 508

AVCO EVERETT RESEARCH LAB INC EVERETT MA  
INVESTIGATION OF THE PRODUCTION OF HIGH DENSITY UNIFORM PLASMAS--ETC(U)  
OCT 80 D H DOUGLAS-HAMILTON, P S ROSTLER F33615-78-C-2013

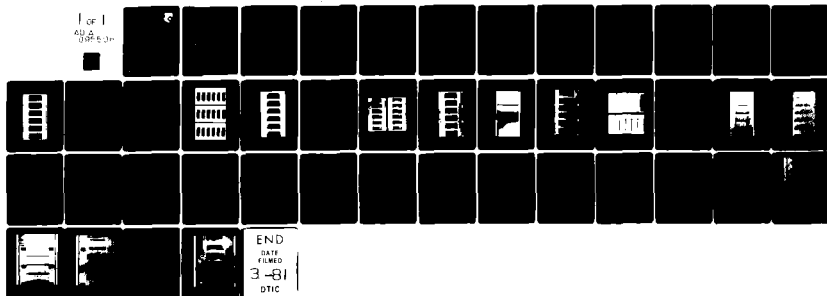
F/G 20/9

UNCLASSIFIED

AFWAL-TR-80-2087

NL

1 of 1  
40 2  
000 5 31



END  
DATE  
FILMED  
3-81  
DTIC

18 AFWAL-TR-80-2087

6 INVESTIGATION OF THE PRODUCTION OF  
HIGH DENSITY UNIFORM PLASMAS,



AD A635508

Avco Everett Research Laboratory, Inc.  
2385 Revere Beach Parkway  
Everett, Massachusetts 02149

10 D. H. / Douglas-Hamilton  
P. C. / Rostler

12 44  
11 Oct 1980  
Technical Report AFWAL-TR-80-2087

9 Final Report, 10 July 1979 - April 1980,

16 2348  
17 S5

15 F 23615-78-C-2413

APPROVED FOR PUBLIC RELEASE; DISTRIBUTION UNLIMITED

DTIC  
FEB 6 1981

FILE COPY

AERO PROPULSION LABORATORY  
AIR FORCE WRIGHT AERONAUTICAL LABORATORIES  
AIR FORCE SYSTEMS COMMAND  
Wright-Patterson Air Force Base  
Ohio 45433

048450


mt

NOTICE

When Government drawings, specifications, or other data are used for any purpose other than in connection with a definitely related Government procurement operation, the United States Government thereby incurs no responsibility nor any obligation whatsoever; and the fact that the government may have formulated, furnished, or in any way supplied the said drawings, specifications, or other data, is not to be regarded by implication or otherwise as in any manner licensing the holder or any other person or corporation, or conveying any rights or permission to manufacture use, or sell any patented invention that may in any way be related thereto.


This report has been reviewed by the Office of Public Affairs (ASD/PA) and is releasable to the National Technical Information Service (NTIS). At NTIS, it will be available to the general public, including foreign nations.

This technical report has been reviewed and is approved for publication.

  
ALAN GARSCADDEN  
Project Engineer

  
ROBERT R. BARTHELEMY  
Chief, Energy Conversion Branch

FOR THE COMMANDER

  
JAMES D. REAMS  
Chief, Aerospace Power Division  
Aero Propulsion Laboratory

"If your address has changed, if you wish to be removed from our mailing list, or if the addressee is no longer employed by your organization please notify AFWAL/POOC, W-PAFB, OH 45433 to help us maintain a current mailing list".

Copies of this report should not be returned unless return is required by security considerations, contractual obligations, or notice on a specific document.

REPORT DOCUMENTATION PAGE		READ INSTRUCTIONS BEFORE COMPLETING FORM
1. REPORT NUMBER AFWAL-TR-80-2087✓	2. GOVT ACCESSION NO. AD A095 508	3. RECIPIENT'S CATALOG NUMBER
4. TITLE (and Subtitle) INVESTIGATION OF THE PRODUCTION OF HIGH DENSITY UNIFORM PLASMAS		5. TYPE OF REPORT & PERIOD COVERED Final Report 10 July 79 - 10 April 80
		6. PERFORMING ORG. REPORT NUMBER
7. AUTHOR(s) D.H. Douglas-Hamilton and P.S. Rostler		8. CONTRACT OR GRANT NUMBER(s) F33615-78-C-2013/
9. PERFORMING ORGANIZATION NAME AND ADDRESS Avco Everett Research Laboratory, Inc.✓ 2385 Revere Beach Parkway Everett, Massachusetts 02149		10. PROGRAM ELEMENT, PROJECT, TASK AREA & WORK UNIT NUMBERS 2308S502
11. CONTROLLING OFFICE NAME AND ADDRESS Aero Propulsion Laboratory (AFWAL/POOC) Air Force Wright Aeronautical Labs. (AFSC) Wright Patterson Air Force Base, Ohio 45433		12. REPORT DATE October 1980
		13. NUMBER OF PAGES 43
14. MONITORING AGENCY NAME & ADDRESS (if different from Controlling Office)		15. SECURITY CLASS. (of this report) Unclassified
		15a. DECLASSIFICATION/DOWNGRADING SCHEDULE
16. DISTRIBUTION STATEMENT (of this Report)  Approved for public release; distribution unlimited		
17. DISTRIBUTION STATEMENT (of the abstract entered in Block 20, if different from Report)		
18. SUPPLEMENTARY NOTES		
19. KEY WORDS (Continue on reverse side if necessary and identify by block number)  E-Beam Discharge Streamers Discharge Stability Laser		
20. ABSTRACT (Continue on reverse side if necessary and identify by block number)  The cathode layer instability which leads to the initiation of streamers in non-self-sustaining discharges is studied by shadow-graph photography. The effects of cathode material and discharge gas composition are investigated. A theoretical model of the instability is formulated and compared with the data. Framing camera color photographs of streamers are obtained and shown to be consistent with a previously developed theory of streamer propagation.		

## FOREWORD

This report was prepared by D.H. Douglas-Hamilton and P.S. Rostler, and describes work which was accomplished at the Avco Everett Research Laboratory, Inc. (AERL), Everett, Massachusetts, under contract F3361578-C-2013 for the Air Force Aero Propulsion Laboratory, Air Force Wright Aeronautical Laboratories, Air Force Systems Command, WPAFB, Ohio 45433. It constitutes Volume II of the Final Report under that contract. The report covers work during the period 10 July 1979 to 10 April 1980, entitled "Investigation of the Production of High Density Uniform Plasmas," under the technical direction of Dr. A. Garscadden, Air Force Aero Propulsion Laboratory.

The technical assistance of Mr. Larry McInnis and Mr. Ed Kierstead is gratefully acknowledged.

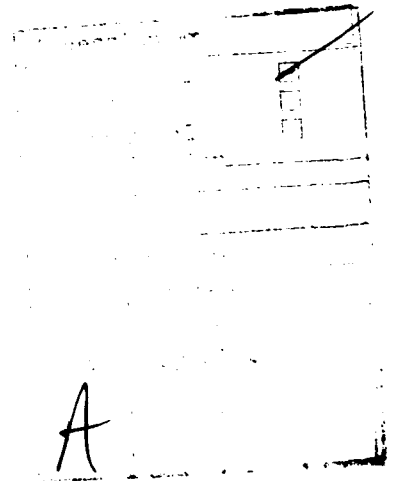


## TABLE OF CONTENTS

<u>Section</u>		<u>Page</u>
I	INTRODUCTION	1
II	EXPERIMENTAL RESULTS	3
	1. Summary	3
	2. Experimental Setup	4
	3. Shadowgraph Data	4
	4. Use of Various Cathode Materials	11
III	ANALYSIS	23
	1. Streamer Growth	23
	2. Streamer Initiation	25
	3. Suppression of Streamers	28
	4. Summary	29
IV	CONCLUSIONS	31
	APPENDIX - COLOR FILMS	32

## LIST OF ILLUSTRATIONS

<u>Figure</u>		<u>Page</u>
1	Shadowgraph Optical System	5
2	A Shadowgraph Sequence Showing the Cathode Layer Instability	6
3	A Sequence of 18 Successive Frames Showing Expansion of the Cathode Layer During and After the E-Beam Pulse	9
4	A Shadowgraph Showing the Cathode Layer Instability in a Discharge in 3-2-1 Gas	10
5	Shadowgraph of a Discharge in 3-1-0.08 Gas	12
6	Cathode Layer Instability with a Chromium-Plated Cathode	13
7	A Photo Sequence Showing Streamer Growth Off a Graphite Cathode	14
8	A Shadowgraph Sequence Taken with the Graphite Cathode	15
9	A Photo Sequence Showing Streamer Growth Off a Copper Cathode	16
10	A Photo Sequence Showing Streamer Growth Off the Dispenser Cathode	18
11	A Photo Sequence Showing Clusters of Streamers Appearing at the Points Where the Kapton Covered Cathode had Arced on the Preceding Run	19
12	Streamer Growth Rate	24
A-1	A Color Photo Sequence Showing Streamers Growing into a Nitrogen Discharge with an Aluminum Cathode (Run #12)	33
A-2	A Color Photo Sequence of a Discharge in 3-1-0.08 Laser Gas with an Aluminum Cathode (Run #14)	34

LIST OF ILLUSTRATIONS (Concluded)

<u>Figure</u>		<u>Page</u>
A-3	Streamer Growth in Nitrogen with a Dispenser Cathode (Run #35)	35
A-4	A Shadowgraph Sequence Taken with Color Film (Run #37)	37



## SECTION I

### INTRODUCTION

Stable, uniform, high density gas discharges have a variety of practical applications. Of particular importance is their use in high-power gas lasers. Such discharges can be made by the e-beam sustainer technique, in which gas ionization is maintained by an externally generated e-beam. This permits operation of the discharge at a voltage below the electron avalanche threshold, where the rapid arc formation seen in higher voltage discharges does not occur. E-beam sustained discharges do form arcs, however, and such arcing is major limitation of devices based on this technology.

The work reported here is a continuation of a study of this arc formation process. As described in Volume I of this report, several instabilities occurring in e-beam sustained discharges were investigated and explained. A major finding was the discovery of discharge streamers, hot filamentary structures which originate at the electrodes (usually at the cathode) and propagate into the discharge.

In the earlier work, the structure and the growth of streamers were studied in a small e-beam sustained discharge apparatus. Detailed, time resolved photographs of streamers were taken with a high-speed framing camera. Streamer growth was found to be exponential, and the scaling of the growth rate with the discharge power was determined. A theoretical model was formulated which gave good agreement with the data. A streamer was described as essentially an arc, a column of hot, conducting gas which carries a concentrated current. The streamer current maintains the streamer temperature and also heats the gas ahead of the streamer, until it too becomes an extension of the streamer column. Thus, the streamer propagates across the discharge, leading eventually to the formation of an arc.

The details of this theoretical description, and the results of the framing camera studies are contained in Volume I. The present volume describes an extension of this work to include the process by which streamers are initiated at the cathode. This has been found to be due to an instability of the cathode layer of the discharge.

A shadowgraph technique has been used to observe the cathode layer instability. Unlike the photographic work reported in Volume I, this technique does not depend upon gas luminosity, and has been used to study the cathode layer instability in various discharge gases. This is a considerable advance over the photographic work, which was limited to the nonlinear phase of streamer growth in nitrogen discharges. The more recent work also included a study of discharges with a variety of cathode materials.

An additional improvement in the diagnostics was the use of color film in the framing camera. This has produced the most detailed photographs of fully developed streamers yet obtained, and provided further confirmation of the theoretical model.

A theory has also been developed for the cathode layer instability seen in the shadowgraph pictures. As explained in more detail below, the basic mechanism is similar to that which drives the streamers in the nonlinear stage. A small protrusion of the cathode layer concentrates the current, heating the gas in the protrusion and causing further expansion. Neither the data nor the calculations are sufficiently detailed for an exact comparison of the growth rate, but the model does predict growth at a rate fast enough to explain the observed rapid development of perturbations of the cathode layer boundary. In some of the shadowgraphs, a well-defined instability wavelength is evident. The wavelength is of the order of the thickness of the cathode layer, which is also consistent with the theory.

Thus, as detailed in the remainder of this report, this extension of the work has led to a reasonable understanding of the streamer initiation process. The new information has important implications for the prevention of arcing in e-beam sustained discharges.

## SECTION II

### EXPERIMENTAL RESULTS

#### 1. SUMMARY

The experimental work described in Volume I has now been extended to include observations of the streamer initiation process and measurements of the effects of different materials and of different gas mixtures in a discharge. For these experiments the framing camera method used in the earlier work has been improved and a new diagnostic, a shadowgraph optical system has been built and added to the mini-bang apparatus. With the shadowgraph technique we were able to observe the cathode layer instability which leads to the formation of streamers. Gas expansion in the cathode layer generates refractive index gradients which will deflect a beam of light, and hence can be seen in shadowgraph photographs. Used in conjunction with the framing camera, this technique has produced time resolved images of the early expansion and initial linear instability of the cathode layer. Both the wavelength and the growth rate of the perturbations can be measured from these photo sequences.

Since this technique does not depend upon gas luminosity, it can be used to study discharges in different gases. In the experiments reported here, the cathode layer instability has been observed in nitrogen, in 3-2-1 laser gas (50% helium, 33.3% nitrogen, 16.7% carbon dioxide) and in 3-1-0.08 laser gas (73.5% nitrogen, 24.5% carbon dioxide, 2% hydrogen).

The effect of differences in cathode material was also examined. Streamer growth was observed for cathodes made of aluminum, copper, stainless steel, graphite, chromium plated aluminum, a dispenser cathode, and a cathode covered with a thin layer of kapton.

The shadowgraph system was gradually improved during the experiments, and in the last few film sequences streamers can be seen. They are not visible in sufficient detail for a quantitative study. With further optical improvements, however, the shadowgraph technique could be used for this purpose as well.

Finally, color photographs of streamers have been taken for the first time with the framing camera. These are a considerable improvement upon the black and white films taken in earlier experiments. The different portions of the streamer structure, which

according to the theoretical model described in Volume I are due to different physical processes, are in fact seen to have different colors. A few of the color photo sequences are included in Appendix A of this report.

Several color film shadowgraphs were also recorded. It was thought that dispersion in the cathode layer might be evident. This in fact was not the case, but these films nevertheless gave the most detailed shadowgraph images obtained in the experiments, due to the higher quality and greater sensitivity of the color film used. One example is included in Appendix A.

## 2. EXPERIMENTAL SETUP

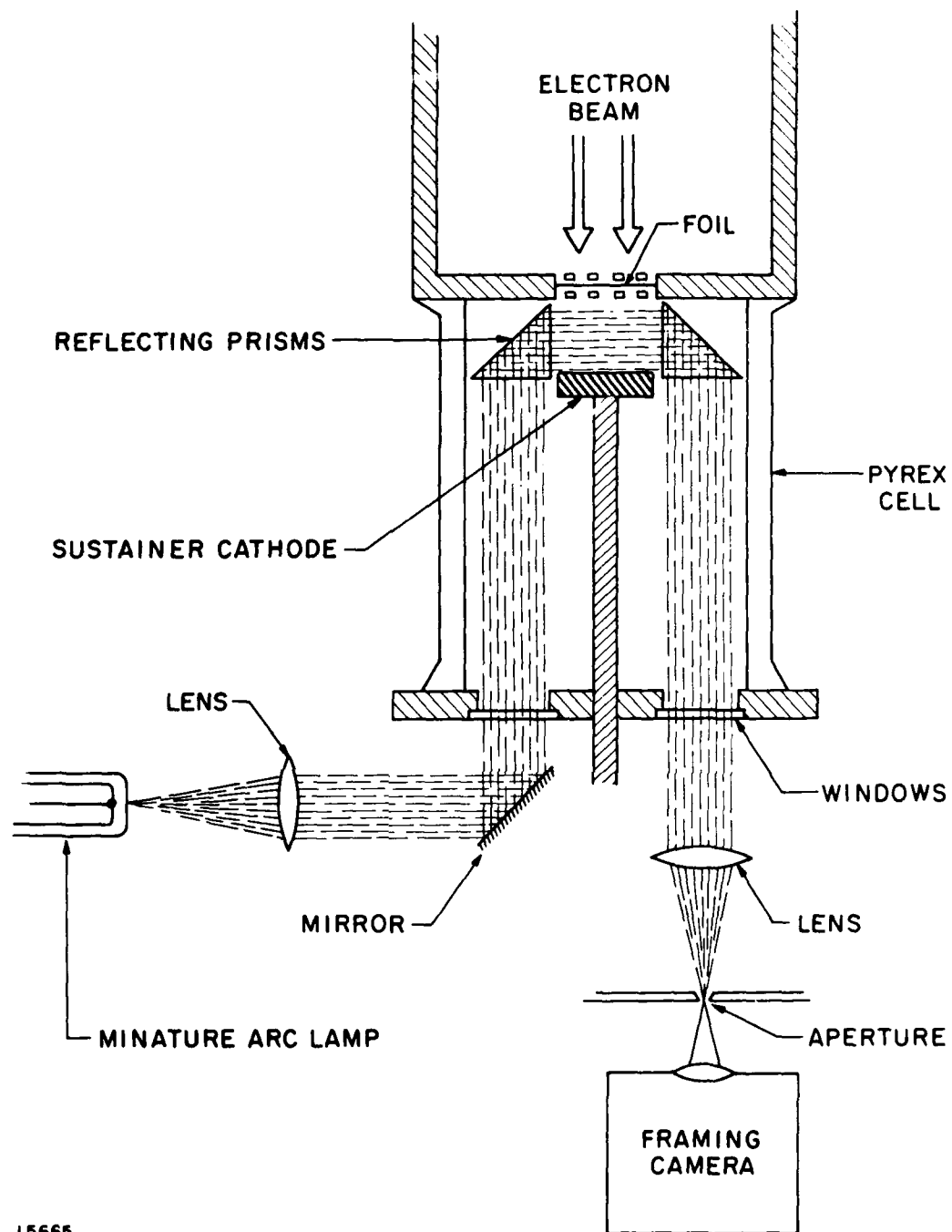
The e-beam discharge apparatus on which these experiments were done was essentially the same as described in Volume I. The principal change since last year's work was the addition of the shadowgraph capability. As shown in Figure 1, a second window and a second reflecting prism were added to the discharge cell. A high brightness dc light source (a Sylvania C25 concentrated arc lamp) and a collimating lens produced a parallel beam of white light which was directed transverse to the discharge. After passage through the discharge region, this light was focused by a second lens onto a small aperture, which was roughly the same size as the focal spot of the beam. That light which passed through the aperture was then observed with the framing camera (a HYCAM high-speed motion picture camera, made by Red Lake Laboratories) which was focused on the discharge. The use of an aperture, of course, gave a large depth of field, so in the shadowgraphs the entire discharge is quite well in focus. The principle of the shadowgraph technique is that a deflection or defocusing of the collimated light by refractive index disturbances in the gas will cause that light to miss the aperture. Hence, the source of the deflection will appear as a dark area or "shadow" on the otherwise uniformly exposed film.\* The same type of film (Kodak RAR film 2498) used in the earlier pictorial work was also used to record the shadowgraphs.

## 3. SHADOWGRAPH DATA

An example of a shadowgraph photo sequence is shown in Figure 2. Six frames are shown and the line of sight is parallel to the surface of the 2 in. square cathode. The cathode surface defines the lower edge of each frame, and the entire width of the cathode is visible. The cathode to anode spacing was one inch. The

---

\* More precisely, a shadowgraph shows defocusing, while observation of deflection gives a schlieren photograph. Since this system is sensitive to both effects, it could be correctly described by either term.



J 5665

Figure 1 Shadowgraph Optical System

RUN I NITROGEN GAS  
ALUMINUM CATHODE SHADOWGRAPH

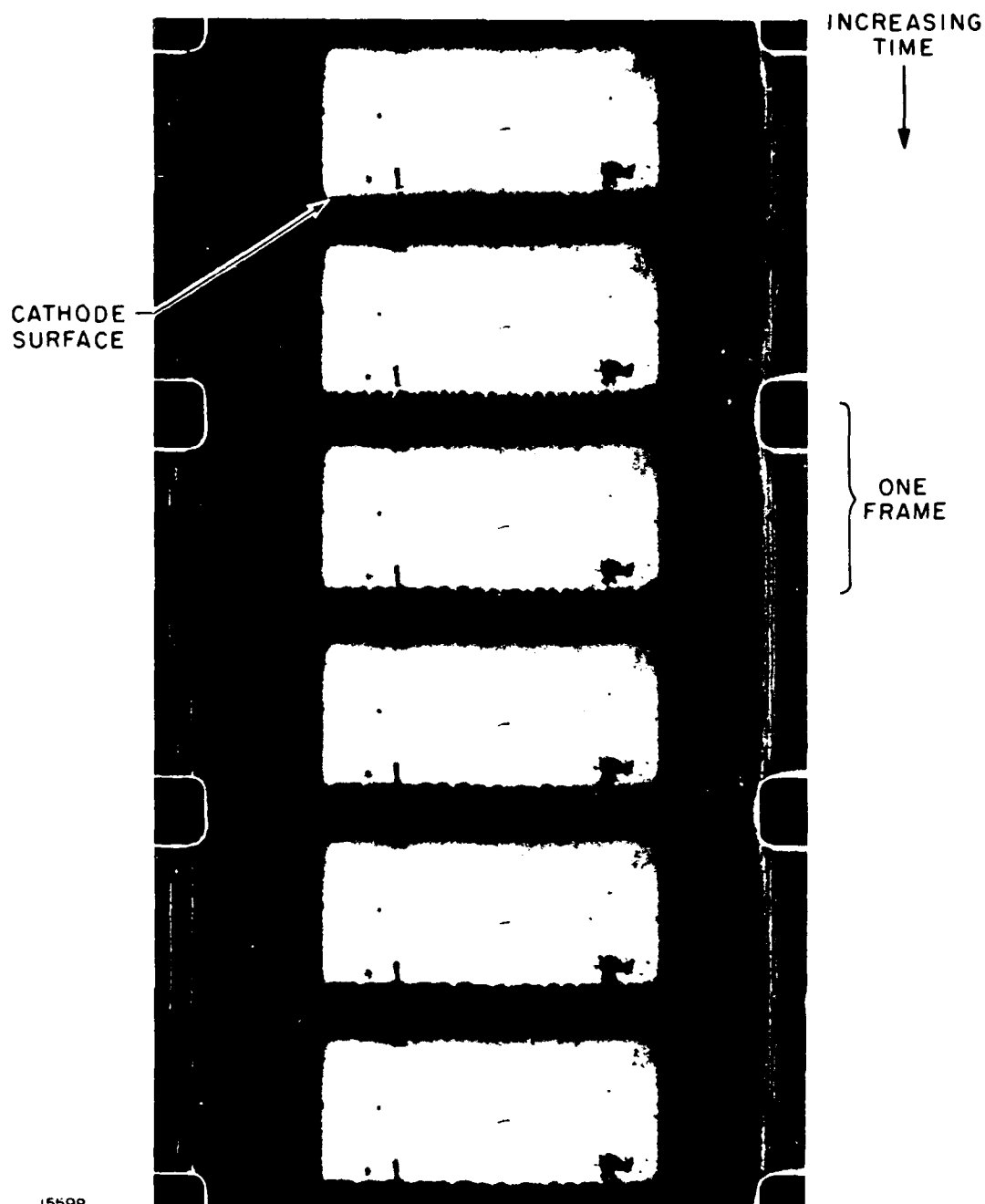


Figure 2 A Shadowgraph Sequence Showing the Cathode Layer Instability

field-of-view extends 0.8 in. from the cathode surface, so the anode is slightly beyond the upper edge of each picture. In this run, the framing rate was 21,000 fps, so the time per frame was 47.6  $\mu$ s. The exposure is 40% of this, i.e., the camera was open for 19  $\mu$ s, closed for 28.6  $\mu$ s, open for 19  $\mu$ s for the next frame, etc.

This discharge was in nitrogen at 760 torr. The measured voltage on the cell was 3.2 kV, and the measured discharge current was 35 A.

The first, i.e., uppermost frame of the sequence was taken before the beginning of the discharge. Any features visible there are due to optical imperfections and should be ignored in all succeeding frames. In the second frame, the cathode layer of the discharge can be clearly seen along the lower edge of the field-of-view. An instability with a well-defined wavelength is evident. Since the view is across the cathode surface, which extends 2 in. along the line of sight, this appearance of a well-defined wavelength in the disturbance implies that the perturbation happened to be oriented with the peaks and valleys parallel to the viewing direction. There is no apparent reason why this should necessarily happen, and in many of the shadowgraphs taken, the instability seems to be oriented differently, but in this particular run the directionality was optimal for observation of the wavelength. As discussed in more detail in Section III, what is seen in these photographs is an unstable expansion of the cathode layer. Early in the pulse a sizable voltage (typically  $\sim 500$  V) is dropped across a thin layer of gas (typically a few hundred mean free paths, or  $\sim 10^{-3}$  cm at atmospheric pressure) at the cathode. Since the power input per unit volume to this gas is much higher than that in the background discharge, the cathode layer is preferentially heated and therefore expands. The shadowgraph data shows that this expansion goes unstable. A possible explanation is that the instability is fluid dynamic - a Rayleigh-Taylor instability which occurs when the hotter, less dense cathode layer gas expands against the more dense background gas. A check of the expected growth rate, however, makes this mechanism improbable, and as noted below, there is evidence that the perturbation growth requires the presence of the discharge current. The fluid-dynamic explanation is probably not correct. The observed instability is in fact driven by the discharge. Provided that the cathode layer voltage drop is roughly constant, a perturbation of the boundary is unstable, because a protrusion of the layer will draw a concentrated current, which preferentially heats the protrusion, causing it to expand further. This model is quantified in Section III. In simplest terms, the conclusion is that the streamer initiation mechanism is essentially the same process which causes streamer growth in the nonlinear regime.

In the third frame of Figure 2, the cathode layer has expanded farther, the instability amplitude has grown, and, interestingly enough, the wavelength of the disturbance has also increased. Apparently, the most unstable wavelength is of the order of the thickness of the cathode layer. As the cathode layer grows, the perturbation shifts to longer wavelengths.

In this run, the e-beam pulse was only 70  $\mu$ s long, so by the fourth frame of the sequence the discharge is over; it did not arc. In the last few frames, the cathode, which is still hot, remains visible, while the perturbation seems to subside gradually.

A more typical run is shown in Figure 3. This discharge was in nitrogen at 8.1 kV, with a 200  $\mu$ s e-beam pulse. (In all the runs taken in this year's experiments, the gas was at atmospheric pressure, and in all except Run 1, the e-beam pulse duration was 200  $\mu$ s. The camera framing rate, which is measured for each run, varied slightly, but was always in the range of one frame every 44.0 - 48.3  $\mu$ s.) Figure 3 shows 18 successive frames of the shadowgraph sequence. Again, the view is parallel to the cathode surface, with the cathode defining the bottom of each frame. The first frame was taken before the discharge. In the second frame, the cathode layer and the instability are evident, although the wavelength is not as easily determined as in Run 1, due presumably to a different orientation of the disturbance. In succeeding frames, the cathode layer and the instability are seen to grow, and, again, the scale of the perturbation also appears to increase as the layer expands.

By the end of the first column of frames, the e-beam pulse is over, and the next two columns show a continued expansion of the hot cathode layer after the discharge. (This discharge did not arc.) Note that this later expansion does not appear to be unstable. In the last few frames shown, the cathode layer appears nearly planar, much more so than during the discharge. This is evidence that the instability is electrical, not fluid-dynamic, because a Rayleigh-Taylor instability would continue to grow during the post-discharge expansion.

A run in a different gas is shown in Figure 4, a shadowgraph of a discharge in 3-2-1 laser gas. The discharge voltage was 9.4 kV and the sustainer current was 30 A. In this mixture, streamers are not bright enough to be seen in direct framing camera photographs. But as is evident from Figure 4, the shadowgraph technique does show the cathode layer instability. The first two frames were taken before the discharge. In the third frame, the instability is visible and the wavelength can be determined. Note that the wavelength is longer near the center of the cathode. This is consistent with the time variations in wavelength seen in Figure 2. Because the e-beam is more intense near the center, the sustainer current and resultant heating of the cathode layer are



RUN 2 NITROGEN GAS ALUMINUM CATHODE SHADOWGRAPH

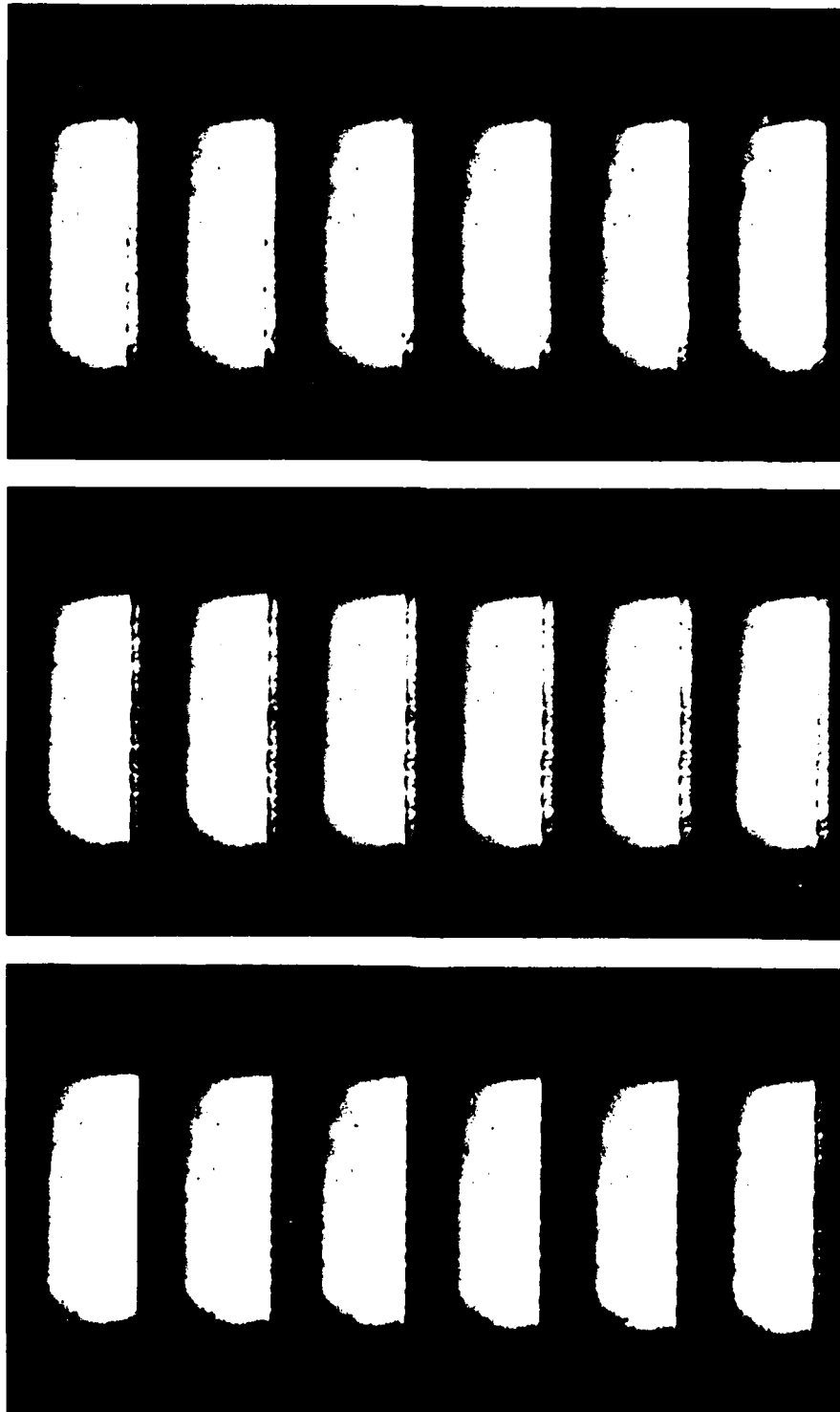
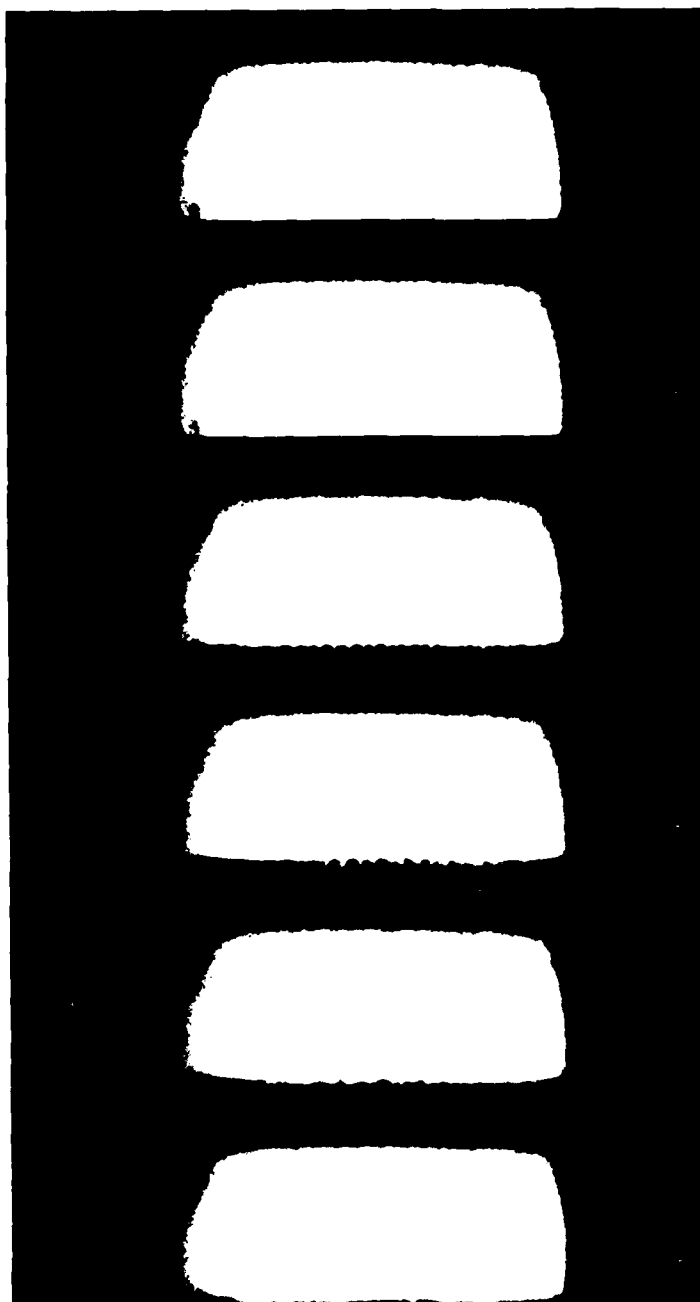


Figure 3 A Sequence of 18 Successive Frames Showing Expansion of the Cathode Layer During and After the E-Beam Pulse

RUN 6 3-2-1 LASER GAS  
ALUMINUM CATHODE  
SHADOWGRAPH



J5594

Figure 4 A Shadowgraph Showing the Cathode Layer Instability  
in a Discharge in 3-2-1 Gas

stronger near the center of the cathode. Hence the cathode layer expansion is fastest there, and the observed longer wavelength of the instability provides further evidence that the scale of the most unstable perturbation varies with the cathode layer thickness.

This discharge did arc 30  $\mu$ s after the end of the e-beam pulse, so by the time of the last few frames in Figure 4, streamers have presumably developed. This probably explains the apparent lessening of the cathode layer instability. In this run, the resolution of the shadowgraph was not quite good enough to see the streamers.

Figure 5 shows a discharge in 3-l-0.08 laser gas. The voltage was 9.7 kV and the sustainer current was 47 A. Here too, the cathode layer instability is evident. This discharge also arced 100  $\mu$ s after the end of the e-beam pulse. The beginning of the arc is visible as a bright spot on the cathode slightly to the right of center in the sixth frame in Figure 5. In the next few frames (not shown here) a very bright arc appears there. This visibility, of course, is not a shadowgraph effect, but just the light emitted by the arc, which is so bright that it can be seen, even through the small viewing aperture used in the shadowgraph system. The second column of frames in Figure 5 is from a much later point on the film. There, the hot gases from the arc can be seen mixing with the colder gas. This sequence is included here because it shows the resolution of the shadowgraph detection system. As evident there, quite fine-scale features can be detected. The reason that the pictures of the cathode layer instability are not so sharp is that the layer moves significantly during the time the camera is open for each frame.

#### 4. USE OF VARIOUS CATHODE MATERIALS

Like the nonlinear streamer growth process, the initial cathode layer instability appears to be driven by current concentrations which cause gas heating which then further concentrates the current. One would expect this to happen in various gases and that is observed to be the case. One would also expect this phenomenon to occur for different cathode materials, and that too is supported by the data. Figures 6-9 show discharges with chromium plated aluminum, graphite, and copper cathodes, all in nitrogen. The discharge in Figure 6 was at 9.7 kV, 67 A, those in Figures 7 and 8 were both at 10.5 kV, 70 A, and that in Figure 9 was at 9.0 kV, 57 A. Figures 6 and 8 are shadowgraph sequences. Figures 7 and 9 are pictorials, i.e., direct photographs similar to those in Volume I. (Conversion of the shadowgraph system to pictorial mode required only shutting off the light source and removing the aperture.) In the shadowgraphs, the cathode layer instability is evident. In the pictorials, the streamer growth is visible. There are indications in the photographs that the graphite cathode reduced the growth of

RUN 10 3-1-.08 LASER GAS  
ALUMINUM CATHODE  
SHADOWGRAPH

~600  $\mu$ SEC AFTER ARC

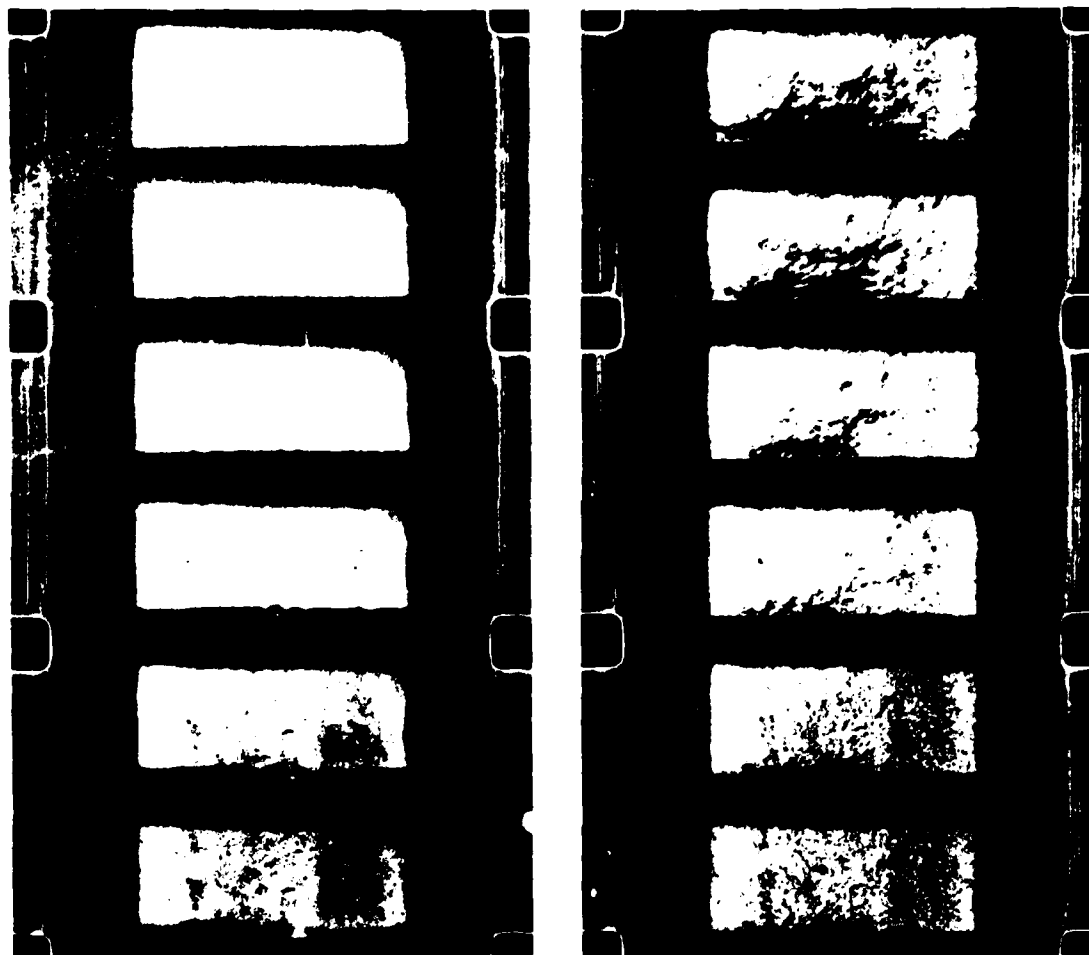
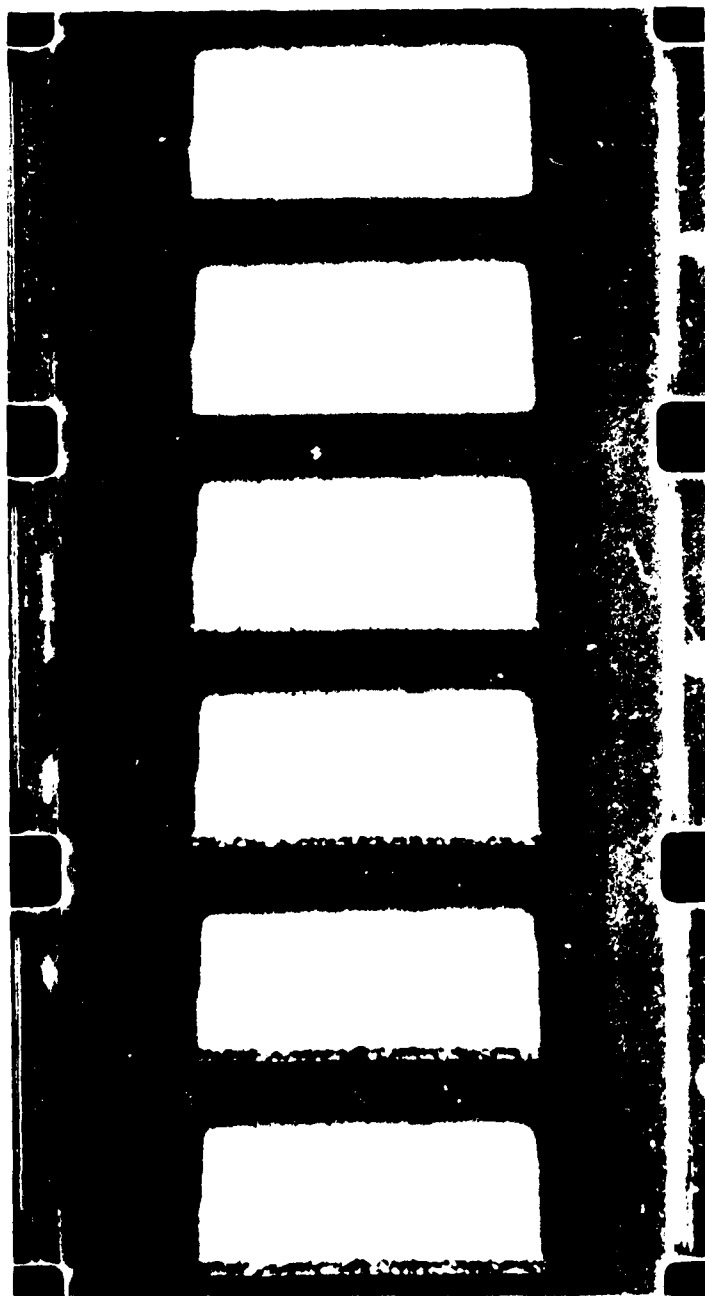


Figure 5 Shadowgraph of a Discharge in 3-1-0.08 Gas. The first sequence shows the cathode layer expansion and instability during the e-beam pulse. The second sequence shows the hot gas 600  $\mu$ s after the discharge arced.

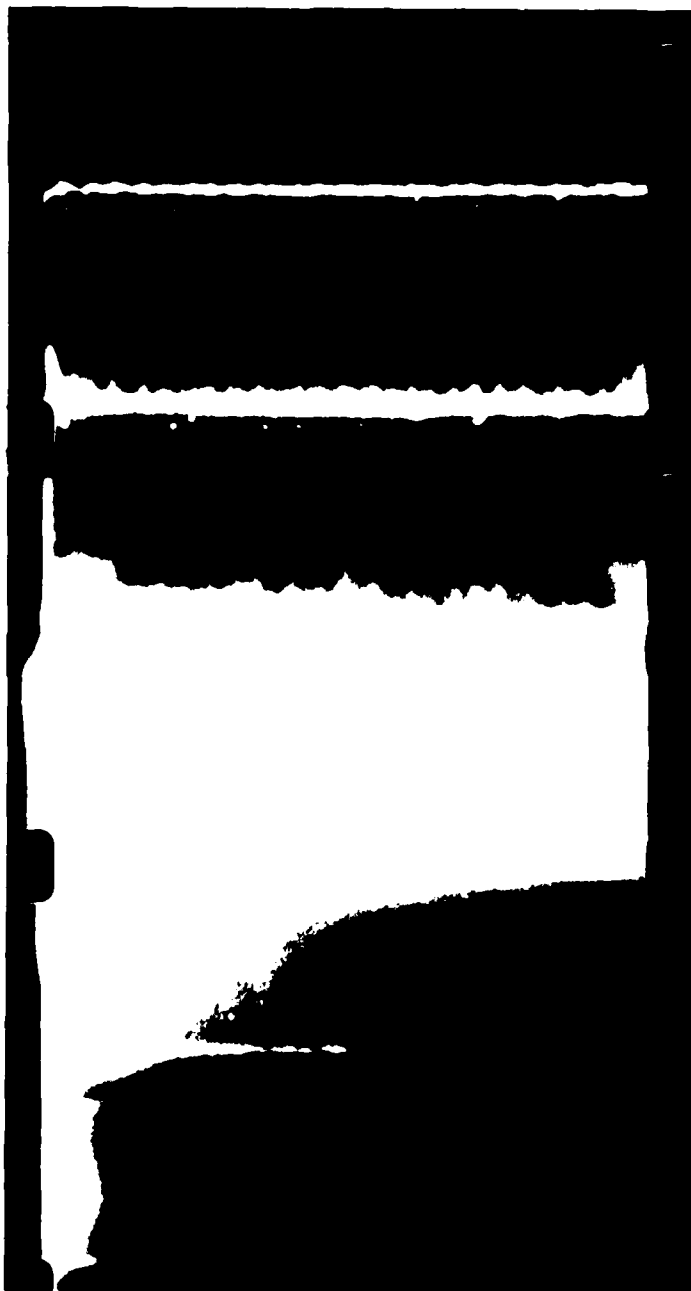
RUN 26 NITROGEN GAS  
CHROMIUM PLATED CATHODE  
SHADOWGRAPH



J5592

Figure 6 Cathode Layer Instability with a Chromium-Plated Cathode

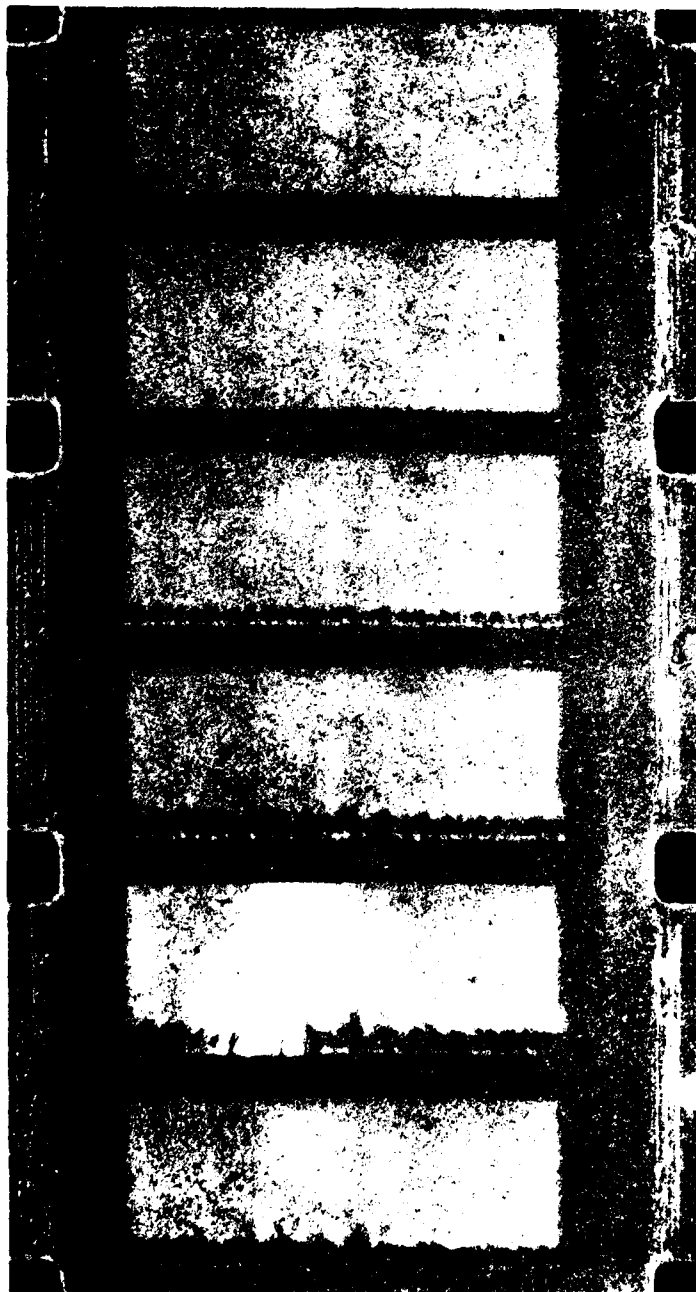
RUN 39 NITROGEN GAS  
GRAPHITE CATHODE  
PICTORIAL



J5595

Figure 7 A Photo Sequence Showing Streamer Growth Off a Graphite Cathode

RUN 40 NITROGEN GAS  
GRAPHITE CATHODE  
SHADOWGRAPH



J5601

Figure 8 A Shadowgraph Sequence Taken with the Graphite Cathode. This run was essentially identical to the one shown in Figure 7.

RUN 42    NITROGEN GAS    COPPER CATHODE    PICTORIAL



J5596

Figure 9    A Photo Sequence Showing Streamer Growth Off a  
Copper Cathode



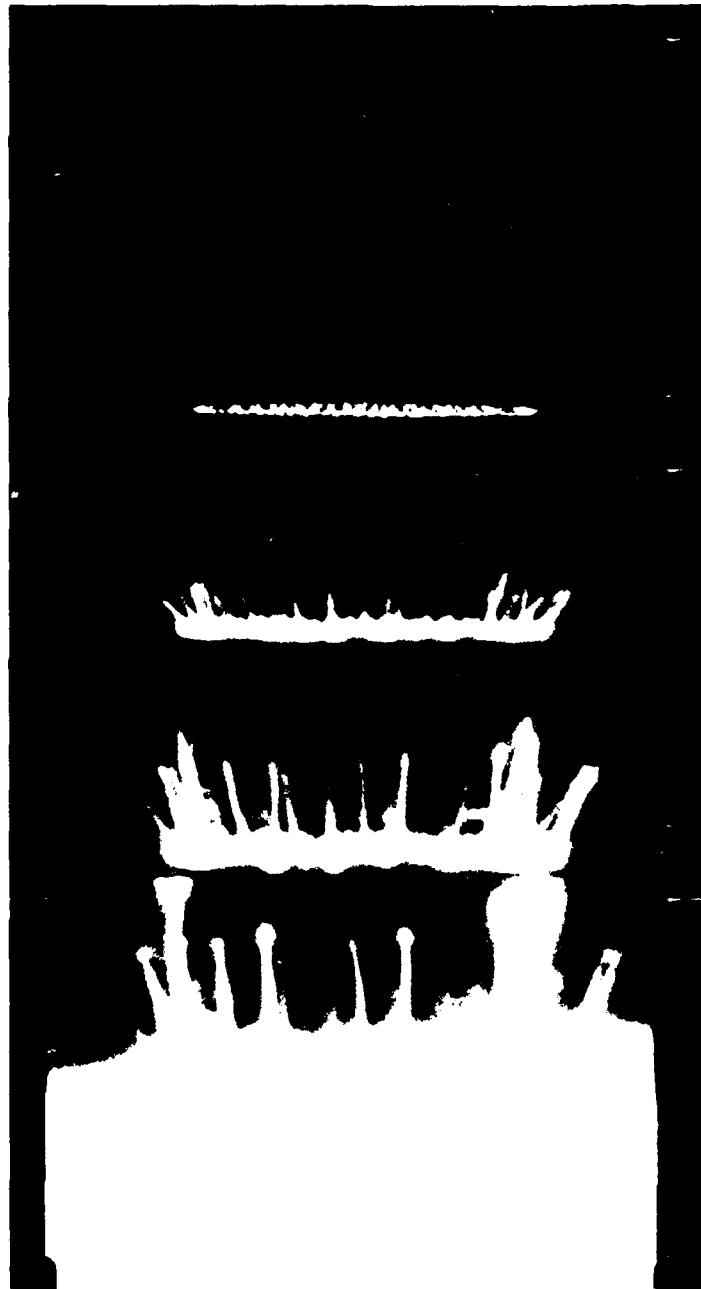
streamers near the center, probably by a ballasting effect of the cathode. These discharges eventually arced at the edge. A more carefully shaped graphite cathode might slightly improve the discharge characteristics, but would be unlikely to suppress the instability for very long.

Figure 9 shows a post-arc. Note that the arc apparently occurred at the center of the discharge. The optical arrangement is such that an arc which appears to be at the center could be at the near or far edge, but from burn marks on the cathodes, it is clear that some arcs did occur near the center. In the early frames of Figure 9, during the e-beam pulse, the largest streamers are seen at the edges, not the center of the discharge. But after the pulse, the streamer at the center continues to grow slowly, leading to a post-arc. (After the pulse, the sustainer voltage is still present. Only the e-beam is pulsed.) An even more pronounced example of this effect is seen in the film (not included here) of Run 43, where a post-arc occurred almost 900  $\mu$ s after the e-beam pulse. In that run, streamers at the cathode edge were almost to the point of arcing when the e-beam terminated, while the only streamers near the center were extremely small - a few millimeters long. Yet the discharge post-arc'd at the center. In the frame before the arc, a streamer can be seen in the center of the cathode. It is evident that differences in residual conductivity of the gas after the pulse due to differences in ionization and heating during the pulse strongly affect the later growth rate of the streamers. This observation is relevant to the problem of downstream arcing in lasers with flowing gases.

A few runs were also taken with a dispenser cathode. It was thought that a cathode with a low work function should give a cathode layer with a lower voltage fall, reducing the gas heating and thus slowing the expansion of the cathode layer. This should delay the onset of the streamer instability. Unfortunately, the dispenser cathode available for the test differed geometrically from the other cathodes which had been used. The dispenser cathode was smaller and had a sharper edge. The result was arcing sooner in the discharge, due to streamers growing rapidly from the edge of the cathode, as can be seen in Figure 10.

Finally, a cathode with a high work function, obtained by covering an aluminum cathode with a kapton foil was run to test the opposite limit. This cathode also arced earlier than the more conventional materials. The first run left several holes in the kapton, and subsequent runs all arced quickly at the same points. An example of this is shown in Figure 11, which shows the effect of severe inhomogeneity in the cathode. We observe in the runs shown earlier that the cathode layer instability grows at wavelengths  $\sim 1$  mm. It seems unlikely that cathode nonuniformities smaller

RUN 33 NITROGEN GAS  
DISPENSER CATHODE  
PICTORIAL



J 5591

Figure 10 A Photo Sequence Showing Streamer Growth Off the  
Dispenser Cathode

RUN 46 NITROGEN GAS  
KAPTON COVERED CATHODE  
PICTORIAL



J5593

Figure 11 A Photo Sequence Showing Clusters of Streamers  
Appearing at the Points Where the Kapton Covered  
Cathode had Arced on the Preceding Run

than this would be important. But one expects larger irregularities to have a large effect, and this borne out by the rapid growth of streamer clusters seen in Figure 11.

During the course of these experiments some pictorials and some shadowgraphs were taken with color film. Examples of the results are included as the Appendix of this report. The most interesting feature in the color pictorials is the difference in color between the core and the halo of streamers in nitrogen. The core is seen to be bluish-white, while the halo is reddish.. It is evident that the cause of the luminosity is different for these regions, as would be expected from the model described in Volume I, probably due to excitation of the nitrogen.

The color film had greater sensitivity than the black and white film, which permitted the shadowgraph system to be aligned for higher resolution. (For a given source brightness, the attainable resolution or angular sensitivity is limited by the required light intensity.) In a color shadowgraph included in Appendix A, fully developed streamers can be seen, showing that with further improvement (in particular, an increased source brightness) the shadowgraph system could be used to study fully developed streamers in various gases.

A total of 46 films were taken in this year's experimental work. A complete list of all the runs, including those discussed above is given in Table 1.

TABLE 1

DATE	5/28/80	5/29/80						5/30/80						6/2/80										
RUN	1	2	3	4	5	6	7	8	9	9A	10	11	12	13	14	15	16	17	18	19	20	21	22	
GAS	NITROGEN				3-2-1					3-1-08		NITROGEN		3-1-08		3-2-1	NITROGEN			3-2-1			3-1-08	
CATHODE	ALUMINUM																							
SUSTAINER VOLTAGE (kV)	3.2	8.0	10.0	10.0	8.1	9.4	9.5	10.2	10.6	9.7	9.7	9.5	9.5	9.5	9.0	9.5	5.5	7.5	9.8	5.0	7.5	9.5	7.9	
SUSTAINER CURRENT DENSITY (A/CM <sup>2</sup> )	1.21	0.56	1.44	1.44	0.90	1.17	---	1.17	1.44	1.76	1.83	1.99	2.15	1.56	1.76	1.56	1.17	1.72	1.95	0.51	0.82	1.40	1.25	
E-BEAM CURRENT DENSITY (mA/CM <sup>2</sup> )	0.96	1.20	1.08	1.10	1.25	1.20	1.08	1.13	1.01	1.15	1.08	1.08	1.08	0.89	0.96	1.03	0.91	0.89	0.77	0.77	0.67	0.91	0.84	
TIME TO ARC (μSEC)	> 70	> 200	135	145	> 200	> 200	> 200	160	160	> 200	> 200	186	185	> 200	> 200	178	> 200	> 200	> 200	> 200	> 200	175	> 200	
ENERGY DEPOSITION (J/CM <sup>2</sup> )	0.11	0.33	0.72	0.77	0.62	0.88	---	0.85	0.96	1.23	1.27	1.19	1.27	1.15	1.24	1.03	0.41	0.84	1.23	0.19	0.50	0.93	0.72	
OPTICAL DIAGNOSTIC	SHADOWGRAPH																							
FILM TYPE	BLACK AND WHITE											PICTORIAL		B & W	COLOR		SHADOWGRAPH							

**J5842**

TABLE 1

**J5841**

### SECTION III

#### ANALYSIS

##### 1. STREAMER GROWTH

In Volume I of this report the subject of streamer growth was discussed and the growth rate of streamers was predicted. It was found that the streamers should grow exponentially and the growth rate  $\gamma$  was derived to be linearly dependent on the mean power input rate per unit volume over the entire discharge, given by

$$\gamma = \frac{3\sigma_o E_o^2}{\lambda k \epsilon} \cdot \frac{a}{c} \left( \frac{7}{4} + \frac{c}{a} \right)^2 \quad (1)$$

where  $\sigma_o$  is positive column conductivity (mho/cm),  $E_o$  is the mean discharge electric field;  $\lambda$  and  $k$  are numerical constants with the value  $\lambda k = 1.04$ ,  $\epsilon$  is the specific energy required to heat a fixed unit volume of gas, while allowing the gas to expand out of the volume, to a sufficient degree of ionization that it becomes conductive [ $\epsilon \cong 1$  J/cm<sup>3</sup> for nitrogen],  $a$  is the streamer halo radius and  $c$  is the streamer length, and the aspect ratio  $a/c$  is approximately constant.

A summary of growth rate measurements for different values of  $E/N$  is shown in Figure 12. The growth rate for discharges in nitrogen at atmospheric pressure  $\gamma$ , in units of inverse 100  $\mu$ s, is shown versus the specific discharge power. It is evident that streamer growth rate increases with power, as predicted by Eq. (1), but the growth rate is slower than the theoretical value, by a factor near 6.

We interpret this as being due to an underestimate of the energy  $\epsilon$  required to raise the temperature to the conductive temperature near 6200°K, for initially the nitrogen will be heated almost entirely in the  $V = 1$  vibrational mode. More than 80% of the discharge energy will be used to excite this first vibrational level due to the high cross section for this mode of excitation. The energy present in the form of vibration, however, is not quenched in pure  $N_2$  at STP for times on the order of minutes. Therefore it is not available for increasing the gas translation temperature, thereby expanding the gas, until the gas temperature has risen sufficiently to raise the  $N_2$  ( $V = 1$ ) collisional deexcitation rate significantly. At very

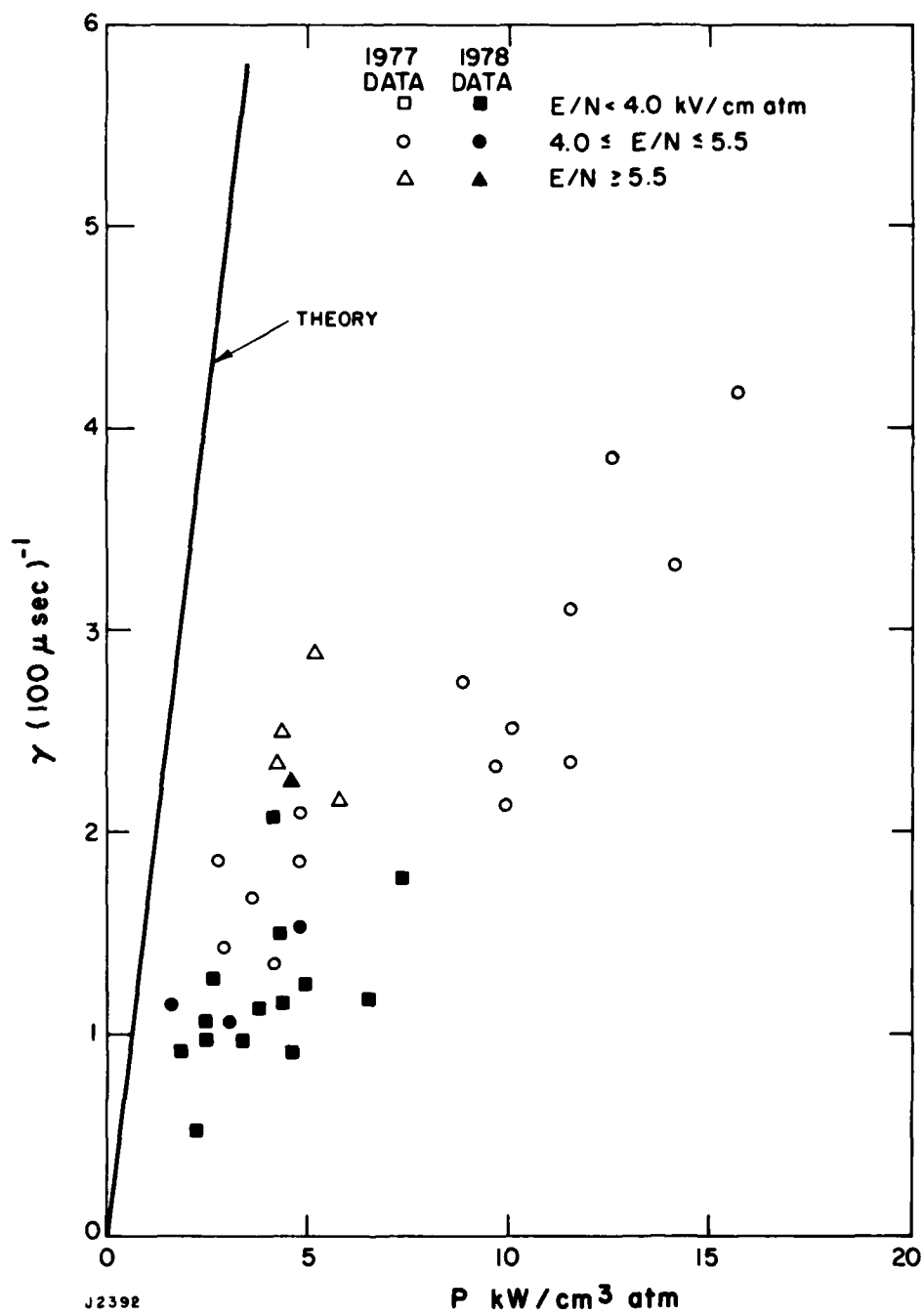


Figure 12 Streamer Growth Rate



high temperatures the deactivation rate becomes large and the energy input is not stored in a metastable vibrational mode, being available for translational heating, dissociation, and ionization. Thus initially the gas does not expand significantly during the discharge. Consequently the value of  $\epsilon \approx 1 \text{ J/cm}^3$  estimated previously is an underestimate, and a better value would be given by assuming that most of the energy ends up in the vibration  $V = 1$  mode until the translational temperature has reached  $\sim 10^3 \text{ K}$ , at which vibrational decay is rapid. Further corrections to the numerical predictions for  $\gamma$  will result from detailed analysis of the streamer head. The essential features of the phenomenon of streamer growth are contained in the present analysis.

## 2. STREAMER INITIATION

The problem of streamer initiation is of extreme importance in nonself-sustaining electric discharges. Once the streamer is formed it grows inexorably with an exponentially increasing velocity, as discussed above. The initiation of the streamer from the cathode is amenable to a simple perturbation analysis. In the present discussion we will concentrate on the cathode layer. Although streamers can and do propagate from anode to cathode, the reverse direction is generally that which leads to arcing, since the cathode layer potential drop is some ten times greater than the anode drop, and consequently initial cathode layer expansion is considerably more violent than anode layer expansion.

Assume that the discharge can be divided into two parts by the cathode front, which expands into the undisturbed discharge due to the intense heating of the cathode layer (CL), and defines the boundary between the cathode layer and the positive column. We will ignore the detailed structure of the cathode layer, which is not essential to this analysis, and simplify the situation by assuming that the CL maintains the same net number of molecules as it expands. This assumption is based on the fact that the physical reason for the CLs existence is to provide sufficient ionizing collisions so that the electron avalanche originating from the cathode can equal in number the positive ions impinging on the cathode. Consequently the number of molecules behind the cathode front (CF) remains constant to first-order.

Perturbing the CF with a wave structure, we describe the shape of the CF as

$$y = y_0 + y_1 \sin kx, \quad (2)$$

where  $x$  and  $y$  are the directions normal and parallel to the electric field, respectively,  $y_1$  is the wave amplitude and  $k$  is the wavenumber. We now assume that the cathode layer region has much

lower resistivity than the positive column. Note that this is only the case after the CL has expanded  $\sim 1$  mm into the discharge: for initially the cathode drop is some 500 V over a distance of  $10^{-3}$  cm, implying a very high resistivity. According to the present model the CF expands (stably at this time) into the positive column. The expansion is stable because protrusions will be less heated than valleys. When the expansion has proceeded to about 1 mm the resistivity in the CL becomes lower than that in the positive column (PC), and the CL will begin to be unstable, since for any protrusion into the PC the heating will be greatest at the protrusion tip, thus causing it to grow faster, a mechanism analogous to that which, at a later stage, results in streamer propagation.

Returning to the perturbation given by Eq. (2), we note that an appropriate solution to Laplace's equation for the potential  $\phi$  when one electrode can be represented by a sine wave is given by

$$\phi = E_0 \left( y - y_1 \sin kx e^{-ky} \right). \quad (3)$$

where  $E_0$  is the initial field: the charge neutrality of the PC allows us to use Laplace's equation to determine the potential. Equation (3) obeys the boundary condition provided  $ky_1 \ll 1$ , with the CF approximately an equipotential, which approximates reality if the resistivity of the CL is low.

The electric field perturbation at the CF peaks will then be

$$E_1 = y_1 k E_0$$

and the corresponding current density perturbations will be

$$J_1 = \sigma y_1 k E_0$$

We can now obtain a growth rate for the perturbation, since by the above assumptions the total mass behind the CF remains constant.

Then the unperturbed distance  $y_B$  from CF to cathode will be

$$y_B = y_0 \rho_0 / \rho$$

where  $y_0$  is the initial value of  $y_B$ . Assuming the perfect gas law, and also assuming that the discharge remains close to isobaric (since otherwise the initial expansion speeds would be sonic or higher, which is not observed), then  $\rho_{B0}/\rho_B = T/T_0$ , where  $T$  is the CL temperature and  $T_0$  is the initial gas temperature. Substitution and differentiation yields

$$\dot{y}_B = y_0 \dot{T}/T_0.$$

The temperature rate of increase is then given by

$$\dot{T} = \frac{J_0 V}{\rho_0 C_p y_0}, \quad (4)$$

where  $V$  is the CL potential drop and  $C_p$  the specific heat. The unperturbed growth rate is then

$$\dot{y}_B = J_0 V / 3.5 k_1 T_0 L \quad (5)$$

where  $k_1$  is Boltzmann's constant and  $L$  the initial gas number density. For a typical discharge,  $J_0 = 5 \text{ A/cm}^2$  and  $V = 500 \text{ V}$ , yielding an expansion velocity near  $7 \times 10^3 \text{ cm/s}$ . The perturbed growth rate will be

$$\dot{y}_1 = J_1 V / 3.5 k_1 T_0 L$$

Hence,

$$\dot{y}_1 = y_1 k \dot{y}_B,$$

which gives the rate of growth of the perturbation compared to the unperturbed rate of growth. We obtain the growth of the perturbation as exponential,  $y_1 = y_{10} e^{\alpha t}$ , where  $\alpha = k \dot{y}_B$ . The unperturbed rate of growth  $\dot{y}_B$  is given by Eq. (5). By determining the wavelength we obtain  $\lambda$ , and hence  $k$ .

We can obtain a minimum wavelength for continued growth by applying the criterion that the characteristic growth time must be faster than the transverse thermal diffusion time. If this were not so the perturbation growth would be damped out by thermal conduction. We write the condition

$$\alpha^{-1} < \frac{(\lambda/2)^2}{\nu},$$

where  $\lambda = 2\pi/k$ , and  $\nu$  is the diffusivity. Then

$$\frac{\lambda}{2\pi \dot{y}_B} < \frac{\lambda^2}{4\nu},$$

or

$$\lambda > \frac{2\nu}{\pi \dot{y}_B}.$$

Since  $\nu \propto \rho^{-3/2}$ , and  $\rho \propto y_B^{-1}$ , we get the condition

$$\lambda > \frac{2}{\pi} \cdot \frac{\nu_0}{\dot{y}_B} \left( \frac{y_B}{y_0} \right)^{3/2} \quad (6)$$

where  $\nu_0$  is the diffusivity at STP.

For the  $N_2$  discharge,  $y_B/y_0 = 100$  for a cathode layer 1 mm thick, and substituting for  $y_B$  from Eq. (5), for typical discharge  $V = 500$  V and  $J_0 = 5$  A/cm<sup>2</sup>, and  $\nu_0 = 0.18$  cm<sup>2</sup>/s we then get

$$\lambda_0 > 0.2 \text{ mm.}$$

Thus for a discharge with a cathode layer already 1 mm thick, perturbations with wavelength greater than the above critical value will grow, while waves shorter than this will be damped. We expect consequently that in the initial stages of expansion of the cathode layer, very short wavelength disturbances will be present, but as the expansion proceeds during the discharge lifetime the larger waves will grow more rapidly. Eventually, of course, the process becomes completely nonlinear and a streamer develops off one of the perturbed peaks, as treated in the previous section.

### 3. SUPPRESSION OF STREAMERS

Note that the growth of the perturbation becomes inevitable under the present model once the resistivity of the region behind

the cathode front is lower than that in the positive column. Thus the cathode layer must be prevented from expanding to the critical thickness at which this becomes true, typically  $\sim 1$  mm. This might be done by convecting the cathode layer out through a hollow or porous cathode. If the cathode layer temperature could be prevented from rising the instability would be prevented: a highly conducting cathode maintained at low temperature might then postpone streamer formation. Unfortunately, this would also produce gas temperature inhomogeneities which would then deleteriously affect the optical quality of the medium, rendering it useless for laser applications. The best method is therefore the first: convective removal of the cathode layer.

#### 4. SUMMARY

In conclusion, a theoretical model of streamer initiation has been derived which gives a physical understanding of the processes present in cathode layer instabilities. Comparison with the shadowgraph experiments obtained on the pulsed e-beam discharge experiment shows that the cathode layer wave perturbations can be observed, that they exhibit a wavelength close to that predicted, with the longer wavelengths dominating at later times, and that they subsequently grow into streamers. We note that this model can be applied to any gas mixture by using the appropriate gas properties.

## SECTION IV

### CONCLUSIONS

In summary, the cathode layer instability which leads to the initiation of streamers in an e-beam sustained discharge has been observed by shadowgraph photography. The instability has been seen to have a well-defined wavelength which increases with increasing thickness of the cathode layer. The cathode layers appear to be consistently unstable for discharges in various gases and for all of the wide variety of cathode materials which were tested.

A theoretical explanation of the instability has been formulated and shown to be consistent with the observations. The instability is driven by the effect of local disturbance in cathode layer thickness upon the cathode layer current distribution, which in turn, affects the heating and expansion of the cathode layer. Since this phenomenon is due to simple electrostatics and to gas heating by the current, one would not expect changes in the gas mixture or the cathode material to have much effect upon the instability. This is borne out by the experimental results.

Since the instability grows with a wavelength of the order of the cathode layer thickness, typically  $\sim 1$  mm, one would also not expect cathode irregularities on a smaller scale to be significant. This conclusion is in contrast to the case of rapid arc formation in high-voltage discharges, where the electric field exceeds the threshold for electron avalanching. There it is known that use of highly polished electrodes is beneficial. No such improvement should be expected for the slower mode of arcing which occurs in lower voltage, e-beam sustained discharges.

There is some evidence from the runs with the graphite cathode that electrical ballasting by the cathode would be helpful. But, this would not eliminate the instability or prevent the eventual formation of arcs. There is also reason to expect that use of a cathode with a low work function would slow the initial instability, but this was not adequately tested, because the dispenser cathode which was used had relatively sharp edges where streamers appeared rapidly.

A more promising approach is use of a porous cathode with gas flow from the discharge into the cathode. The propagation of the instability at early stages is much less than sonic, so an incident

gas flow might keep the disturbances out of the main volume of the discharge. An examination of this possibility could be the subject of a future research effort.

The use of color photography has further confirmed the streamer model discussed in Volume I. The very different appearance of the streamer stem and halo is consistent with the analysis which shows that the streamer stem consists of hot gas while the halo is due to nonthermal excitation of cooler gas.

Finally, the experiments have shown that the shadowgraph technique could, with further refinement, be used to study fully developed streamers in discharges in various laser gas mixtures.

## APPENDIX

### COLOR FILMS

The most detailed pictures of streamers were obtained by using color film (Kodak Ektachrome Vidio News Film 7250) in the framing camera. Figure A-1 shows a framing sequence of a discharge in nitrogen. In color, the difference between the streamer stem and halo is pronounced. The stem, which we believe to be very hot gas, appears bluish-white. The halo, which we believe to be due to non-thermal excitation and ionization by the strong electric field around the streamer tip, is reddish-orange. One can see that initially the luminosity is confined to a very thin sheath at the electrode.

Figure A-2 shows a discharge in 3-1-0.08 laser gas. There, streamers are not visible, and the reddish emission is suppressed, even though this gas too consists primarily of nitrogen. This discharge did arc - in the center of the field-of-view - and we believe that streamers did produce the arc, but are not seen because the streamer temperature is lower in a gas with a lower ionization potential. The absence of nonthermal emission, the reddish halo, is probably due to collisional quenching of the upper state of the transition by the  $\text{CO}_2$  or  $\text{H}_2$  in the mixture. In the last few frames before the arc, bluish emission is seen from the gas above the cathode. In these views the camera is looking through 2 in. of such gas, so emission can be seen at a level which in a streamer would not be recorded.

Figure A-3 shows another discharge in pure nitrogen, in this case with a dispenser cathode. The entire upper surface of the cathode, which is smaller than the cathode in Figures A-1 and A-2, can be seen. The cathode is a solid cylinder, with a flat circular upper surface facing the discharge. The view is slightly down onto this surface. In the first frame the cathode surface is visible as a white luminous disc. (The row of bluish dots below the bright region is due to emission from a fine groove around the side of the cylinder just below the upper surface.) In this sequence, the streamer structure is particularly evident. The streamers appear to originate at the edge of the cathode, probably due to the local field concentrations.

Note that the streamers first bend out, following the electric field and current lines, but then curve inward, toward the region of stronger e-beam generated excitation and ionization. In the



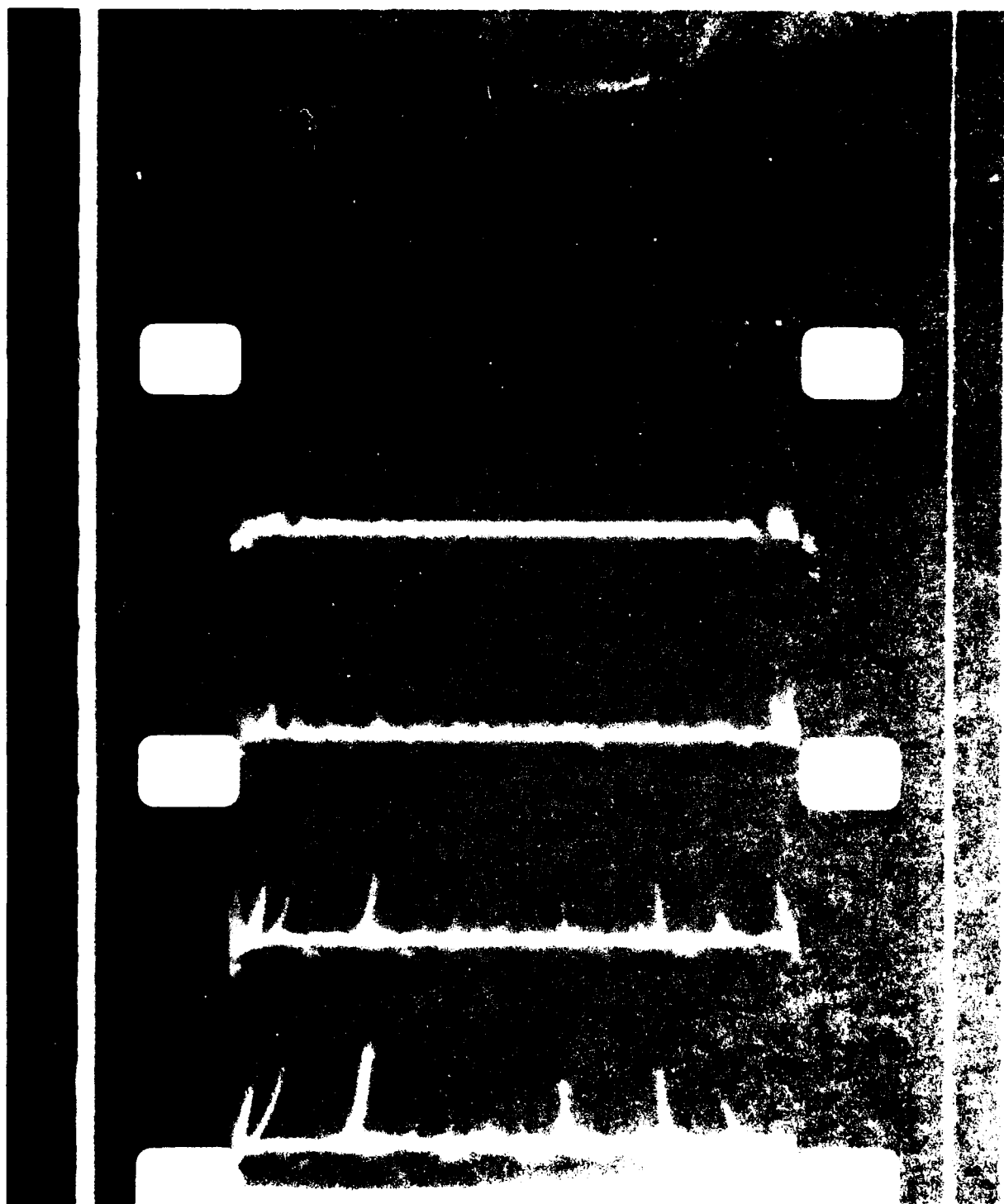


Figure A-1 A Color Photo Sequence Showing Stages Growing from a Cathode Discharge with an Aluminum Cathode (Run #1)

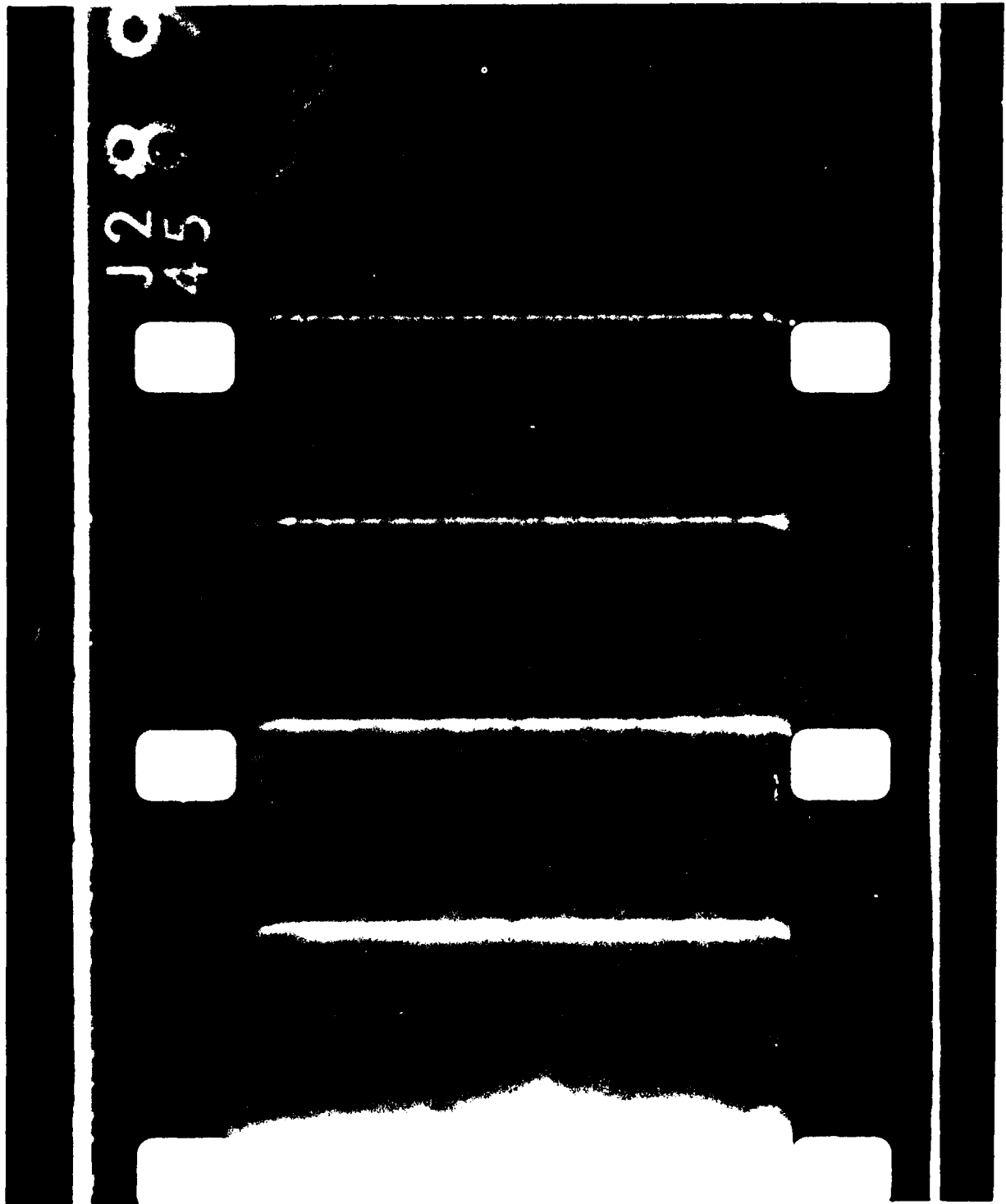


Figure A-2 A Color Photo Sequence of a Discharge in 3-1-0.0% Laser Gas with an Aluminum Cathode (Run #14)

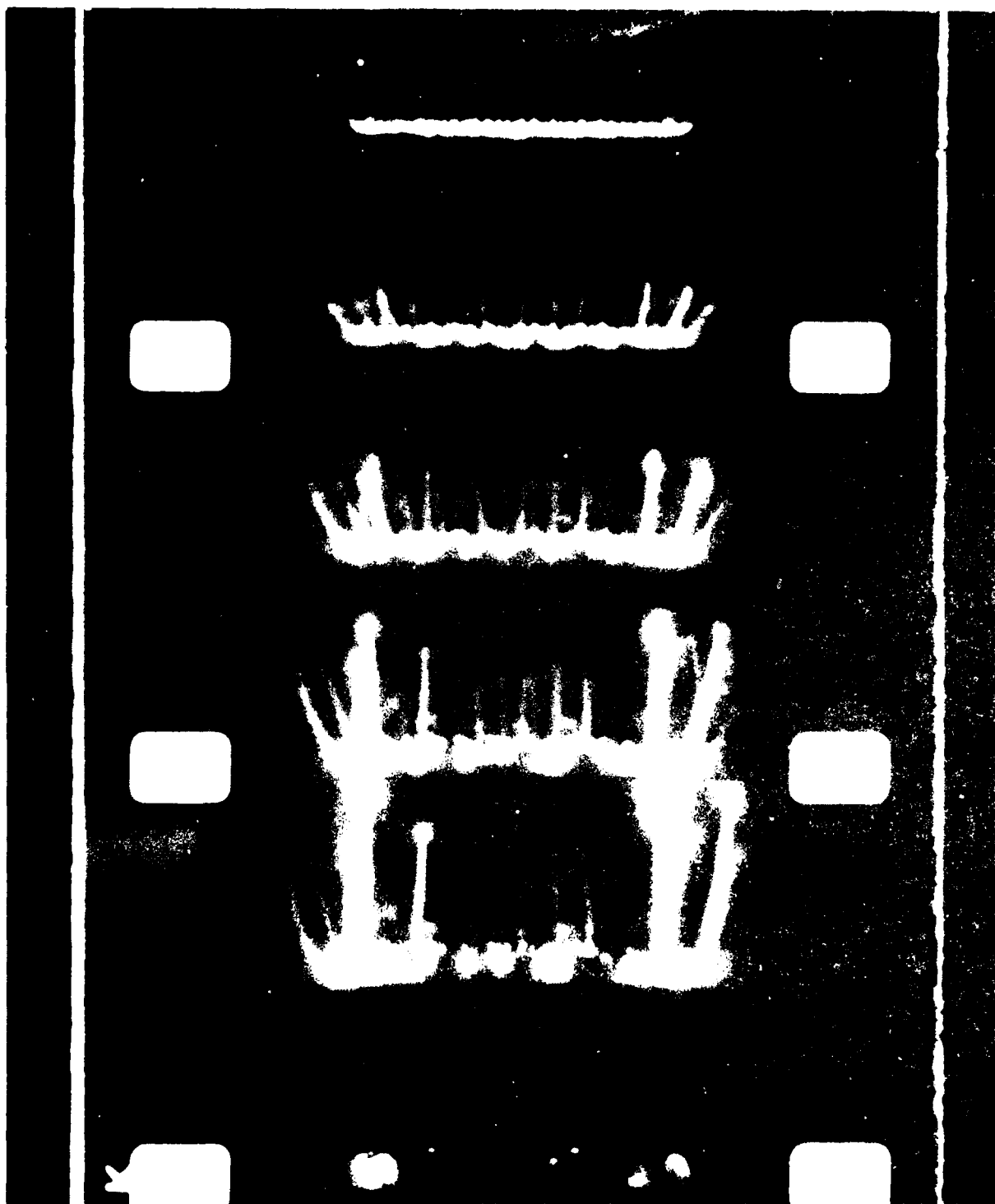


Figure A-3 Streamer Growth in Nitrogen with a Dispenser Cathode  
(Run #35)

last frame shown, the e-beam pulse has ended and the streamers have dimmed, but not disappeared. This discharge post-arc'd at the right-hand edge of the cathode 225  $\mu$ s after the end of the e-beam pulse, as can be seen in later frames not included here.

Finally, more shadowgraphs were also taken using color film. The best example is shown in Figure A-4. This is also a nitrogen discharge with the dispenser cathode. Because the color film is more sensitive than the black and white film used, it permitted an increase in the deflection sensitivity of the optical arrangement. The result is that fully developed streamers can be seen. The resolution is still not sufficient for detailed analysis, but this film does show that with further refinement, the technique could be used for this purpose.

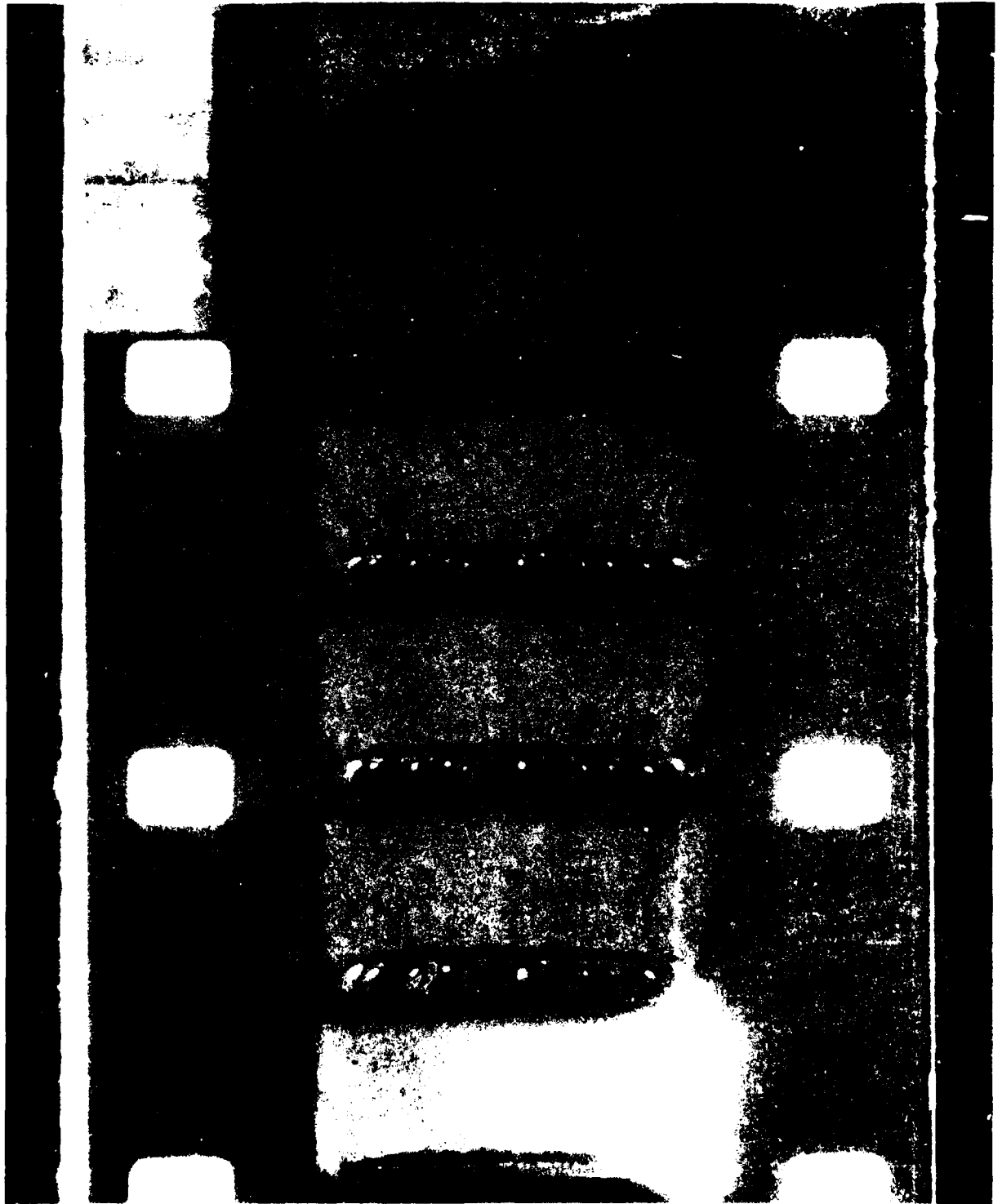


Figure A-4 A shadowgraph Sequence Taken with Color Film (Run #32)